

Rethinking Glaucoma Calibration: Voting-Based Binocular and Metadata Integration

Taejin Jeong¹ Joohyeok Kim¹ Jaehoon Joo¹ Yeonwoo Jung² Hyeonmin Kim²
Seong Jae Hwang¹ *

¹Yonsei University ²Medi Whale

Abstract. Glaucoma is an incurable ophthalmic disease that damages the optic nerve, leads to vision loss, and ranks among the leading causes of blindness worldwide. Diagnosing glaucoma typically involves fundus photography, optical coherence tomography (OCT), and visual field testing. However, the high cost of OCT often leads to reliance on fundus photography and visual field testing, both of which exhibit inherent inter-observer variability. This stems from glaucoma being a multi-faceted disease that influenced by various factors. As a result, glaucoma diagnosis is highly subjective, emphasizing the necessity of calibration, which aligns predicted probabilities with actual disease likelihood. Proper calibration is essential to prevent overdiagnosis or misdiagnosis, which are critical concerns for high-risk diseases. Although AI has significantly improved diagnostic accuracy, overconfidence in models have worsen calibration performance. Recent study has begun focusing on calibration for glaucoma. Nevertheless, previous study has not fully considered glaucoma’s systemic nature and the high subjectivity in its diagnostic process. To overcome these limitations, we propose V-ViT (Voting-based ViT), a novel framework that enhances calibration by incorporating disease-specific characteristics. V-ViT integrates binocular data and metadata, reflecting the multi-faceted nature of glaucoma diagnosis. Additionally, we introduce a MC dropout-based Voting System to address high subjectivity. Our approach achieves state-of-the-art performance across all metrics, including accuracy, demonstrating that our proposed methods are effective in addressing calibration issues. We validate our method using a custom dataset including binocular data.

Keywords: Glaucoma · Model Calibration · Binocular Data · Metadata

1 Introduction

Glaucoma currently affects 80 million people worldwide and is a leading cause of blindness, with incidence on the rise [23]. Due to its asymptomatic nature, glaucoma frequently remains undiagnosed in its early stages, resulting in significant vision impairment and increasing the treatment costs for advanced cases [19]. Consequently, early detection is essential to preventing blindness and reducing financial strain. Diagnosing glaucoma typically involves a multi-faceted approach,

* Corresponding author.

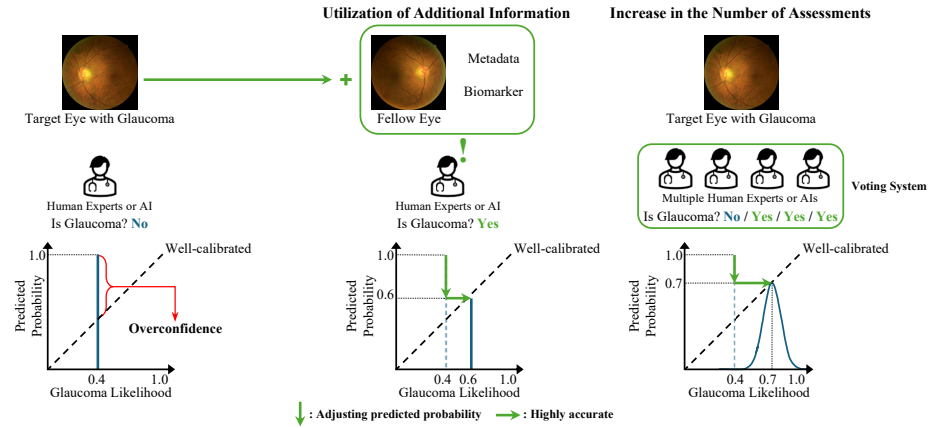


Fig. 1. The impact of binocular data, metadata, and the Voting System on calibration. Integrating glaucoma-relevant information and multiple predictions influences diagnostic accuracy and adjusts predicted probabilities, thereby enhancing model calibration.

including fundus photography, optical coherence tomography (OCT), and visual field testing. Among these methods, OCT is expensive, so the early diagnosis of glaucoma primarily relies on fundus photography and visual field testing. However, because glaucoma is a multi-faceted disease, these two diagnostic methods inevitably involve inter-observer variability [2,3,13,10,22]. Therefore, the combination of high risk and high subjectivity emphasizes the need for robust model calibration in glaucoma.

Model calibration is the process of adjusting a model’s predicted probabilities to align with the actual likelihood of being correct. Consequently, various methods—temperature scaling, label smoothing, and loss function adjustments—have been proposed to achieve this alignment [8,15,18,1]. As model accuracy continues to improve, the need for uncertainty quantification (UQ) is becoming increasingly important. UQ is the process of systematically estimating the confidence or uncertainty in a model’s predictions, which is especially critical in the medical field where misinterpretations can have severe consequences. In medical applications, accuracy alone does not map directly to the reliability of AI predictions; their predicted probabilities must align with the actual probability of correctness, making proper calibration essential for clinical deployment. Overconfidence in the presence of disease can lead to unnecessary examinations and treatments, increasing healthcare costs, while overconfidence in its absence may cause clinicians to overlook the disease. Ensuring that predicted probabilities accurately reflect actual probabilities is even more important. Although study on calibration for glaucoma diagnosis has recently begun [24], previous study has not fully considered the unique characteristics of glaucoma, emphasizing the need for new approaches tailored to this disease. Therefore, we address the cali-

bration problem by leveraging the fact that glaucoma is a systemic disease and the inter-observer variability in its diagnosis [20,14,17,6].

To begin with, glaucoma is a systemic disease. Consequently, a comprehensive evaluation allows for a more accurate diagnosis and effective management, since this requires considering not only ocular imaging but also systemic health factors. For example, diabetes, hypertension, and systemic inflammation can all influence glaucoma [25,9]. Furthermore, the condition of the fellow eye, along with patient’s age, sex, race, genetics, and lifestyle factors, has also been associated with glaucoma [21,12,26]. Notably, studies show that many unilateral glaucoma patients eventually experience bilateral disease, with up to 41.67% of cases affecting both eyes over time [16]. Age and sex are also risk factors, with older individuals and men at greater risk. Therefore, we argue that integrating glaucoma-relevant information would resolve calibration issues, as illustrated in Fig. 1. For instance, if an overconfident model learns from the fellow eye and finds that it does not have glaucoma, it will lower its confidence, considering the bilateral nature of the disease.

In addition, inter-observer variability in glaucoma diagnosis leads to high subjectivity. Indeed, relying on a single ophthalmologist’s diagnosis as the dataset label poses a significant risk. Instead, depending on the multiple trusted specialists can reduce the influence of any one ophthalmologist. As shown in Fig. 1, we propose that this approach can indirectly achieve label-smoothing benefits while mitigating human variability, ultimately enhancing calibration performance.

To address the aforementioned issues, we introduce three novel approaches. First, we integrate binocular data by incorporating a Cross-Attention (CA) block into the ViT model [5]. Second, we concatenate age and sex information into the patch embeddings. Third, to minimize the risk of misdiagnosis, we consult 1 to 18 trusted ophthalmologists and create a custom dataset labeled with the averaged values of their assessments. Based on this, we implement a MC dropout-based Voting System. Further details on the dataset are provided in Sec. 3.

Our contributions: **(1)** We address the calibration problem by leveraging the characteristics of glaucoma through binocular data and metadata; **(2)** We propose a new method for processing metadata and biomarkers, which offers easy plug-and-play integration in transformer-based models; **(3)** We propose a new task to address calibration in highly subjective diagnosis and introduce a Voting System as a solution, along with a new framework, V-ViT (Voting-based ViT).

2 Methodology

Fig. 2 shows our proposed framework, V-ViT. In the following sections, we introduce metadata tokens that integrate additional information and CA blocks that capture and fuse complementary information from the fellow eye (Sec. 2.1). Then, we present an MLP-based Voting System (Sec. 2.2).

2.1 Utilizing Glaucoma-Relevant Information

Incorporating Patient Metadata for Glaucoma. As mentioned in Sec. 1,

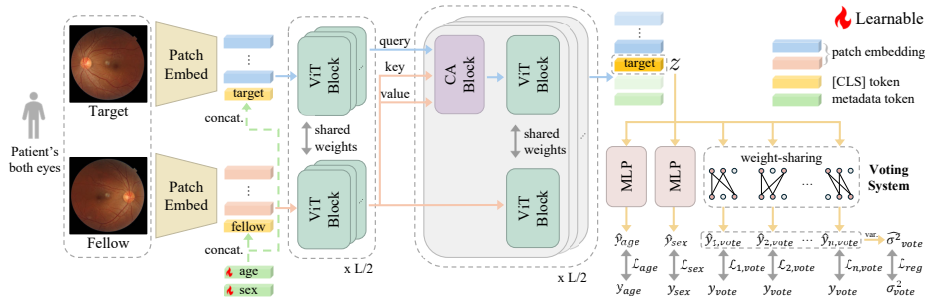


Fig. 2. Overview of V-ViT. Through a total of L ViT blocks and $L/2$ CA blocks, V-ViT learns to incorporate the fellow image and metadata for glaucoma diagnosis.

various factors influence glaucoma. To account this characteristic, we propose learnable metadata tokens to utilize patient’s metadata alongside fundus images. Inspired by previous study demonstrating that additional register tokens enhance model performance [4], we randomly initialize each metadata token with the same dimension as the image embeddings and integrate its corresponding metadata by multiplying it with the actual metadata value. Similar to the [CLS] token in ViT, these tokens are concatenated with the patch embeddings of the input images.

We employ age and sex information as metadata and biomarker, which are easily obtainable and associated with glaucoma. During training, these learnable tokens are optimized to obtain the optimal representation of the input metadata. They participate in the attention operation with the image tokens, allowing metadata information to be propagated to image tokens and enabling the model to incorporate metadata for glaucoma diagnosis. This token-based approach is highly scalable, allowing seamless adaptation to additional metadata and biomarkers without requiring significant architectural modifications.

Fusing Information from the Fellow Eye. Given the bilateral nature of glaucoma, we propose the CA block that captures and integrates complementary information from the fellow eye. Leveraging the capability of the attention layer to learn relationships between image tokens, the proposed CA block, which consists of a multi-head attention layer is designed to establish connections between the target and fellow fundus images, enabling the detection of clinical signs that cannot be identified in a unilateral image. Specifically, the attention’s query is derived from the target image, while the key and value are obtained from the fellow image. This allows the attention mechanism to generate a fellow-aware target embedding.

2.2 Reliable Diagnosis via a Voting System

Considering the high subjectivity in glaucoma diagnosis, the reliability of the diagnosis improves as the number of assessments increases. Similarly, we aim to obtain more reliable diagnostic outputs through iterative computations rather

than a single inference. For the i -th prediction, the final [CLS] token representation z is fed into an MLP-based Voting System, which generates the predicted probability of glaucoma, $\hat{y}_{i,vote}$. Instead of relying on a single prediction, multiple predictions are obtained for the same image.

To ensure variability in each prediction, dropout in the Voting System is activated during both training and inference phases, as introduced in Multi-sample dropout [11] and MC dropout [7], respectively. The activated dropout randomly selects a subset of weights from the Voting System, inducing changes in the focused features. This approach enables the model to mimic the voting process among multiple ophthalmologists, thereby improving diagnostic reliability. Since our dataset contains the averaged assessments from 1 to 18 ophthalmologists as label data, denoted as y_{vote} , $\hat{y}_{i,vote}$ can be directly evaluated against the label data. Thus, we define \mathcal{L}_{vote} for model training using the MSE loss.

$$\mathcal{L}_{vote} = \frac{1}{n} \sum_{i=1}^n \mathcal{L}_{i,vote}, \quad \mathcal{L}_{i,vote} = \mathbb{E}[\|y_{vote} - \hat{y}_{i,vote}\|_2^2], \quad (1)$$

where n represents the number of times multiple predictions are performed.

Additionally, we utilize two linear layers to predict the patient’s age and sex from z . This process encourages the model to encode metadata within the [CLS] token, facilitating the effective fusion of metadata and image tokens. We apply MSE loss for age prediction and cross entropy loss for sex classification, where each loss is weighted by a factor, λ_{age} and λ_{sex} , derived from its association with glaucoma. The overall loss function for model training is defined as follows:

$$\mathcal{L}_{total} = \mathcal{L}_{vote} + \lambda_{age}\mathcal{L}_{age} + \lambda_{sex}\mathcal{L}_{sex} + \lambda_{reg}\mathcal{L}_{reg} + \lambda\|\theta\|^2. \quad (2)$$

\mathcal{L}_{reg} is a regularization term that adjusts the variance of the Voting System outputs to match the variance of assessments from multiple ophthalmologists, denoted as σ_{vote}^2 in Fig. 2. $\lambda\|\theta\|^2$ is introduced to impose a prior on θ in the context of Bayesian deep learning, where θ represents the parameters of V-ViT. λ is given as the weight decay coefficient for the parameter θ .

3 Experiments

Dataset and Preprocessing. We used data collected from 14 medical institutions, including the UK Biobank, with each dataset labeled by 1 to 18 ophthalmologists. After preprocessing, we obtained 7,213 pairs of binocular data and 5,343 single-eye samples, resulting in a total of 19,769 samples. For single-eye samples, the same eye image as the target was assigned to the fellow position to construct the dataset. Among them, 15,815 samples were used for the training and validation dataset, while 3,954 samples were allocated to the test dataset.

Implementation Details. All experiments ran on a single NVIDIA RTX A6000 Ada GPU. We used a ViT-Tiny pretrained on ImageNet. For the first stage of training, we trained only the newly added layers for the first 10 epochs, and then trained the entire model. We used $n = 8$ and a dropout rate of 0.3 in Voting System, allowing label variance in the validation set to emerge probabilistically.

Table 1. Quantitative evaluation of V-ViT performance compared to Vijayan et al., including results from the ablation study. Bolded values mark the best performance. (B: Binocular data, M: Metadata, and V: Voting System, respectively; * uses V-ViT but replaces the fellow eye image with the target image.)

Model	B	M	V	Recall \uparrow	F1 \uparrow	ECE \downarrow	MSE \downarrow	ACC \uparrow
Vijayan et al. [24]				0.662	0.705	0.050	0.063	0.869
Vanilla ViT-T		✓		0.675	0.725	0.031	0.056	0.880
			✓	0.698	0.731	0.025	0.056	0.879
		✓	✓	0.697	0.733	0.019	0.056	0.880
V-ViT (Ours)			✓	0.703	0.738	0.021	0.055	0.883
	*			0.690	0.723	0.021	0.057	0.875
	*		✓	0.675	0.725	0.030	0.058	0.880
	*	✓		0.694	0.725	0.018	0.058	0.876
	*	✓	✓	0.706	0.737	0.015	0.055	0.881
	✓			0.706	0.745	0.033	0.053	0.886
	✓		✓	0.708	0.745	0.027	0.055	0.886
	✓	✓		0.744	0.756	0.017	0.054	0.887
	✓	✓	✓	0.750	0.761	0.010	0.052	0.889

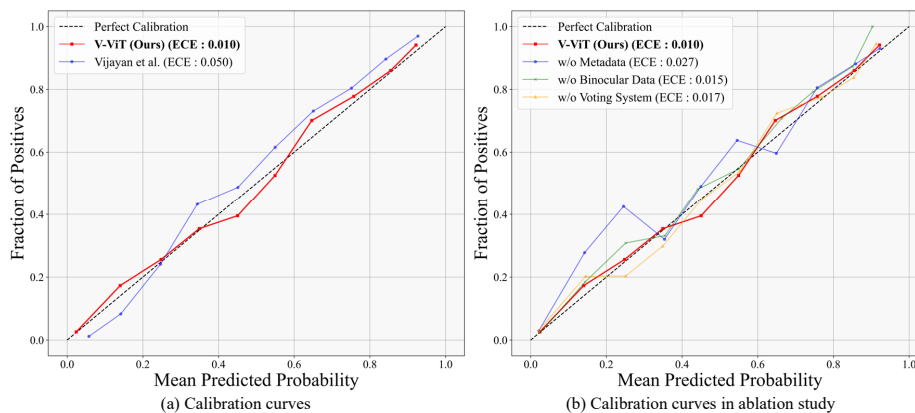


Fig. 3. (a) The calibration curves comparing the model proposed by Vijayan et al. with V-ViT. (b) The calibration curves from the ablation study.

3.1 Quantitative Results

Table 1 compares V-ViT with those from previous study using evaluation metrics commonly employed in medical calibration tasks. We use Recall, F1 score, Expected Calibration Error (ECE), MSE, and Accuracy (ACC). ECE indicates the gap between predicted probability and actual accuracy. We achieve state-of-the-art results on all metrics. Misdiagnosis in high-risk diseases can be critical, making Recall and ECE essential metrics. Therefore, these results validate the effectiveness of our method, as it is both safer and more accurate.

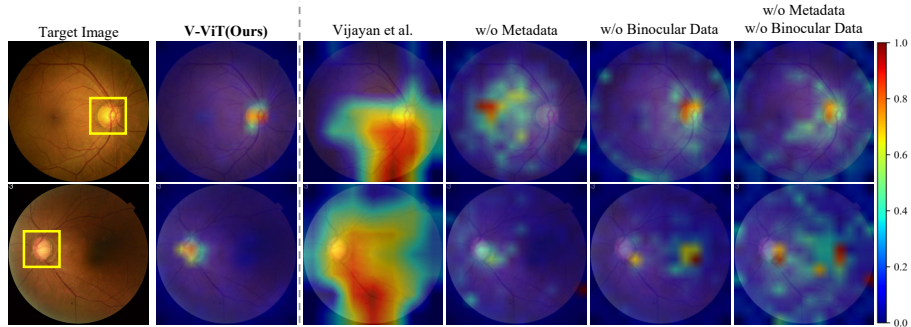


Fig. 4. Attention map for the target image. The yellow boxes on the target image indicate the regions that should be focused on for glaucoma diagnosis.

For metrics that require binary information (e.g., disease presence), we assign 1 if the predicted or label value is 0.5 or higher, and 0 otherwise. Fig. 3(a) presents the calibration curves comparing the model proposed by Vijayan et al. with V-ViT, where better calibration is indicated by a curve closer to $y = x$. As a result, the results show that V-ViT achieves superior calibration.

3.2 Ablation Study

Table 1 compares the quantitative results based on the use of binocular data, metadata, and the Voting System. We also evaluate the performance of vanilla ViT-Tiny (ViT-T) using only the target image. Fig. 3(b) illustrates calibration curves based on whether metadata, binocular data, and the Voting System are used. Each model removes just one of these three components. The results show that applying our techniques leads to improved performance.

Attention Map. Fig. 4 illustrates the attention map obtained using the final [CLS] token. For simplicity, we visualize the attention map without corners considering attention sink [27]. The yellow boxes indicate the optic disc and optic cup, which are used for glaucoma diagnosis in fundus images. When our proposed methods are applied, the model tends to focus more precisely on clinically significant regions that ophthalmologists typically observe. Therefore, this suggests its potential as an assistance tool that emphasizes key areas for ophthalmologists to focus on during diagnosis, while also providing better interpretability.

3.3 Calibrating Confidence

We hypothesized that incorporating binocular data and metadata would adjust the model’s output and yield superior calibration performance. For instance, if the model predicts that the target eye is not glaucoma but the fellow eye is glaucoma, the calibration process assigns higher confidence. To validate the hypotheses, we conduct three experiments.

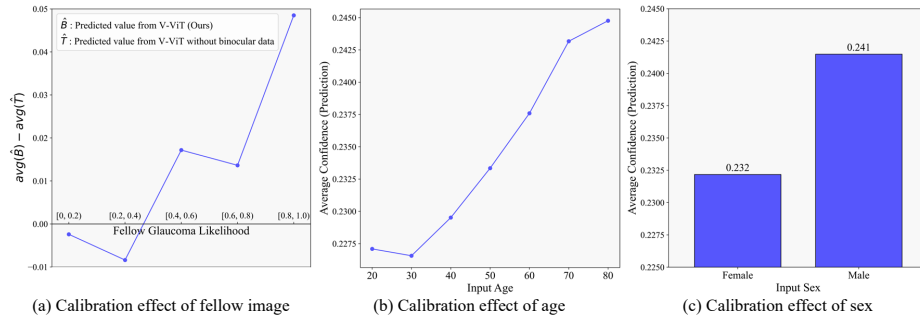


Fig. 5. (a) The average prediction difference based on the fellow eye’s label. (b) Inference results when setting all individuals’ ages to 20–80. (c) Inference results when setting all individuals’ sex to female and male.

Calibration Effect of Fellow Images. Fig. 5(a) illustrates how binocular data influence the model’s output. \hat{T} denotes the predicted value from a model trained without binocular data, and \hat{B} denotes the predicted value from our proposed model. We plot the difference between obtained by subtracting the average of \hat{B} and \hat{T} according to the glaucoma likelihood of the fellow image. If the likelihood of glaucoma in the fellow eye, the \hat{B} value becomes smaller. Conversely, if the fellow eye is more likely to have glaucoma, \hat{B} becomes higher. These results capture the bilateral nature of glaucoma and corroborate our hypothesis.

Calibration Effect of Metadata. Fig. 5(b) shows how the **age** affects the model’s output. At inference, we overrode the age values across the test dataset, ranging from 20 to 80, and observed the changes in predictions. As the assigned age increased, the model’s predicted values also increased, demonstrating that the model correctly reflects clinical findings from previous studies [21]. Similar to age, we set the **sex** to female and male in the test dataset and compared the results, as shown in Fig. 5(c). This result is consistent with clinical findings that show a higher incidence of glaucoma in males [12]. Through these two results, we confirm that metadata significantly influences the model’s predictions, demonstrating the efficacy of our metadata processing method.

4 Conclusions

This study emphasizes the importance of calibration in glaucoma diagnosis. By integrating binocular information and metadata into our V-ViT, we effectively capture the bilateral and multi-faceted nature of the disease. Additionally, we introduce an MC dropout-based Voting System to mitigate overconfidence, thereby enhancing model reliability. These findings suggest that calibration not only improves diagnostic confidence but also enables safer and more efficient glaucoma diagnosis in clinical settings.

References

1. Barfoot, T., Garcia Peraza Herrera, L.C., Glocker, B., Vercauteren, T.: Average calibration error: A differentiable loss for improved reliability in image segmentation. In: International Conference on Medical Image Computing and Computer-Assisted Intervention. pp. 139–149. Springer (2024)
2. Blumberg, D.M., De Moraes, C.G., Liebmann, J.M., Garg, R., Chen, C., Thevenithiran, A., Hood, D.C.: Technology and the glaucoma suspect. *Investigative ophthalmology & visual science* **57**(9), OCT80–OCT85 (2016)
3. Chou, J.Y., Tseng, P.C., Hu, H.Y., Yen, C.Y.: Intraocular pressure and optical coherence tomography concerning visual field outcomes in “green” patients: An observational study. *Medicine* **103**(46), e40518 (2024)
4. Darcet, T., Oquab, M., Mairal, J., Bojanowski, P.: Vision transformers need registers. arXiv preprint arXiv:2309.16588 (2023)
5. Dosovitskiy, A.: An image is worth 16x16 words: Transformers for image recognition at scale. arXiv preprint arXiv:2010.11929 (2020)
6. Fingert, J.: Primary open-angle glaucoma genes. *Eye* **25**(5), 587–595 (2011)
7. Gal, Y., Ghahramani, Z.: Dropout as a bayesian approximation: Representing model uncertainty in deep learning. In: international conference on machine learning. pp. 1050–1059. PMLR (2016)
8. Guo, C., Pleiss, G., Sun, Y., Weinberger, K.Q.: On calibration of modern neural networks. In: International conference on machine learning. pp. 1321–1330. PMLR (2017)
9. Hsu, E., Desai, M.: Glaucoma and systemic disease. *Life* **13**(4), 1018 (2023)
10. Iester, M., Capris, E., De Feo, F., Polvicino, M., Brusini, P., Capris, P., Corallo, G., Figus, M., Fogagnolo, P., Frezzotti, P., et al.: Agreement to detect glaucomatous visual field progression by using three different methods: a multicentre study. *British Journal of Ophthalmology* **95**(9), 1276–1283 (2011)
11. Inoue, H.: Multi-sample dropout for accelerated training and better generalization. arXiv preprint arXiv:1905.09788 (2019)
12. Kapetanakis, V.V., Chan, M.P., Foster, P.J., Cook, D.G., Owen, C.G., Rudnicka, A.R.: Global variations and time trends in the prevalence of primary open angle glaucoma (poag): a systematic review and meta-analysis. *British Journal of Ophthalmology* **100**(1), 86–93 (2016)
13. King, A., Farnworth, D., Thompson, J.: Inter-observer and intra-observer agreement in the interpretation of visual fields in glaucoma. *Eye* **11**(5), 687–691 (1997)
14. Kubota, R., Noda, S., Wang, Y., Minoshima, S., Asakawa, S., Kudoh, J., Mashima, Y., Oguchi, Y., Shimizu, N.: A novel myosin-like protein (myocilin) expressed in the connecting cilium of the photoreceptor: molecular cloning, tissue expression, and chromosomal mapping. *Genomics* **41**(3), 360–369 (1997)
15. Müller, R., Kornblith, S., Hinton, G.E.: When does label smoothing help? *Advances in neural information processing systems* **32** (2019)
16. Nam, J.W., Kang, Y.S., Sung, M.S., Park, S.W.: Clinical evaluation of unilateral open-angle glaucoma: a two-year follow-up study. *Chonnam Medical Journal* **57**(2), 144 (2021)
17. Rezaie, T., Child, A., Hitchings, R., Brice, G., Miller, L., Coca-Prados, M., Héon, E., Krupin, T., Ritch, R., Kreutzer, D., et al.: Adult-onset primary open-angle glaucoma caused by mutations in optineurin. *Science* **295**(5557), 1077–1079 (2002)
18. Sambyal, A.S., Niyaz, U., Shrivastava, S., Krishnan, N.C., Bathula, D.R.: Ls+: Informed label smoothing for improving calibration in medical image classification.

- In: International Conference on Medical Image Computing and Computer-Assisted Intervention. pp. 513–523. Springer (2024)
19. Soh, Z., Yu, M., Betzler, B.K., Majithia, S., Thakur, S., Tham, Y.C., Wong, T.Y., Aung, T., Friedman, D.S., Cheng, C.Y.: The global extent of undetected glaucoma in adults: a systematic review and meta-analysis. *Ophthalmology* **128**(10), 1393–1404 (2021)
 20. Stone, E.M., Fingert, J.H., Alward, W.L., Nguyen, T.D., Polansky, J.R., Sunden, S.L., Nishimura, D., Clark, A.F., Nystuen, A., Nichols, B.E., et al.: Identification of a gene that causes primary open angle glaucoma. *Science* **275**(5300), 668–670 (1997)
 21. Tham, Y.C., Li, X., Wong, T.Y., Quigley, H.A., Aung, T., Cheng, C.Y.: Global prevalence of glaucoma and projections of glaucoma burden through 2040: a systematic review and meta-analysis. *Ophthalmology* **121**(11), 2081–2090 (2014)
 22. Tielsch, J.M., Katz, J., Quigley, H.A., Miller, N.R., Sommer, A.: Intraobserver and interobserver agreement in measurement of optic disc characteristics. *Ophthalmology* **95**(3), 350–356 (1988)
 23. Velpula, V.K., Sharma, L.D.: Multi-stage glaucoma classification using pre-trained convolutional neural networks and voting-based classifier fusion. *Frontiers in Physiology* **14**, 1175881 (2023)
 24. Vijayan, M., Prasad, D.K., Srinivasan, V.: Advancing glaucoma diagnosis: Employing confidence-calibrated label smoothing loss for model calibration. *Ophthalmology Science* **4**(6), 100555 (2024)
 25. Wändell, P., Carlsson, A.C., Ljunggren, G.: Systemic diseases and their association with open-angle glaucoma in the population of stockholm. *International ophthalmology* pp. 1–9 (2022)
 26. Wang, X., Chen, W., Zhao, W., Miao, M.: Risk of glaucoma to subsequent dementia or cognitive impairment: a systematic review and meta-analysis. *Aging Clinical and Experimental Research* **36**(1), 172 (2024)
 27. Xiao, G., Tian, Y., Chen, B., Han, S., Lewis, M.: Efficient streaming language models with attention sinks. *arXiv preprint arXiv:2309.17453* (2023)